

Optimization Design and Research on Vibration and Noise of Permanent Magnet Synchronous Motor for Vehicle

Jun Shen^{1, *}, Xuejun Chen^{2, *}, Zhixin Cui¹, and Lin Ma¹

Abstract—The electromagnetic vibration noise level of a permanent magnet synchronous motor (PMSM) directly affects the Noise, Vibration, and Harshness (NVH) performance of an electric vehicle. Taking a PMSM for electric vehicle driving as an example, the electromagnetic noise characteristics were studied by combining ANSYS Workbench multi-physical field finite element analysis platform. The electromagnetic vibration force of the stator teeth of the motor is the main source of electromagnetic noise. The magnetic field of the motor can be optimized by changing the slot structure of the motor rotor, so as to improve the electromagnetic vibration force of the stator teeth and reduce the electromagnetic vibration noise of the motor. In order to optimize the magnetic field, three different rotor slot structures are proposed. The most suitable slot structure is found by comparing and analyzing the magnetic field, noise field, and electromagnetic force with the structure before optimization. By comparing the results before and after optimization, it can be seen that the optimized motor can effectively reduce the vibration noise of the motor and ensure the electromagnetic performance of the motor.

1. INTRODUCTION

Permanent magnet synchronous motors for vehicles have the characteristics of light weight, high efficiency, simple structure, stable operation, etc. They have been widely used in new energy vehicles under major brands. As people's requirements for environmental sound in driving are getting higher and higher, Noise, Vibration, and Harshness (NVH) performance indicators of new energy vehicles play an increasingly important role in the competition in the automotive industry.

Different from traditional automobiles, electric motors have replaced internal combustion engines as the main source of automobile power. Therefore, many scholars have gradually turned their attention to the optimization of NVH performance of automobile motors.

Motor noise includes structure noise and control power noise. The vibration noise of permanent magnet synchronous motors for new energy vehicles is mainly caused by electromagnetic noise under structure noise. Many scholars have done some research on the electromagnetic noise of motors.

In the early structure design, Ref. [1] achieved the purpose of changing the electromagnetic excitation force of the stator teeth by optimizing the rotor magnetic isolation bridge structure, thereby reducing the vibration and noise of the motor. Ref. [2] proposed a structure of stator tooth tip arc offset, which offsets the original tooth tip arc along the radial direction to the outer diameter of the stator for a certain distance to improve the stator magnetic density distribution, make the force uniform, and reduce vibration. Ref. [3] started from the stator tooth chamfering, analyzed the air gap flux density expression of the fractional slot permanent magnet synchronous motor when the stator tooth chamfered, and calculated the harmonic amplitudes under different tooth chamfering angles. Finally, the finite element method and analytical formula are used to calculate and analyze the influence of the tooth chamfering method on the electromagnetic vibration and noise of the motor. Jafarboland and

Received 27 October 2020, Accepted 21 December 2020, Scheduled 13 January 2021

* Corresponding author: Jun Shen (sjun1995@foxmail.com), Xuejun Chen (cxjnet@126.com).

¹ School of Mechanical Engineering and Automation, Fuzhou University, Fuzhou 350108, China. ² School of Mechanical and Electrical Engineering, Putian University, Putian 351100, China.

Farahabadi [4] optimized the stator yoke thickness (D) and slot angle (A) related parameters of the stator slot to maximize the stator natural frequency without changing the slot area and stator outer diameter. In terms of stator slot inclination, a lot of research has been done. Zhu et al. [5] studied the different types of different oblique poles: non-inclined pole, two-segment oblique pole, four-segment oblique pole, and oblique slot. The radial electromagnetic force waves and electromagnetic noise under the rotor segmented oblique poles are studied. The study found that when the order of the tooth harmonics was an integer multiple of the segment number, the rotor oblique poles could not attenuate the tooth harmonics of this order. When it was a non-integer multiple, the order of tooth harmonics could be effectively suppressed, and electromagnetic noise was significantly reduced. Both Lee et al. of Qiming University in South Korea and Lin et al. of Tongji University [6, 7] analyzed the deflection angle of the stator slot, using Ansys and LMS Virtual-lab simulation analysis tools, respectively, and obtained an optimal deflection angle. The basic model and tilt model were tested for vibration and noise. The comparison between the simulation results and the actual test results of the model verifies the validity of the analysis structure. Ref. [8] compared the noise performance of the motor under different stator skew factors. After choosing the best stator structure, the acoustics of the permanent magnet synchronous motor was tested to further verify the simulation analysis results. In the research of [9], the rotor is divided equally along the axial direction, and each stepped rotor is designed with a different inclination angle. This structural layout is similar to the effect of offset stator slots, which can effectively weaken the tooth resonance of the motor wave and improve the torque ripple of the permanent magnet synchronous motor.

In the later stage of motor control, Ref. [10] studied the influence of the saturation flux density harmonics at the low-speed and large-load operating point and the magnetic flux density harmonics generated by the magnetic field distortion caused by the high-speed field weakening operation on the electromagnetic noise of the motor. Starting from the theory of digital pulse width modulation (PWM), motor vibration and noise can also be researched and optimized. Zhang et al. [11] proposed a new method that combines dual-branch three-phase permanent magnet synchronous motor with carrier phase shift technology to achieve complete reduction of odd-order PWM frequency vibration. Hara et al. [12] studied the influence of electromagnetic force on circuit noise. It is found that electromagnetic noise and vibration are caused by the radial electromagnetic force generated in the space 0-order mode of $f_{c+}/-3f_1$ and $2f_c$ (f_c : carrier frequency, f_1 : current fundamental frequency). It is shown that the radial electromagnetic forces of $f_{c+}/-3f_1$ and $2f_c$ are caused by PWM harmonics. At the same time, the $1/f_c$ voltage reference update time has a significant effect on the radial electromagnetic force of the frequency f_c . Refs. [13, 14] also adopted the control technology based on digital pulse width modulation (PWM) and mainly proposed a digital PWM speed regulation technology based on proportional integrator (PI). Through simulation, the digital PWM controller and rapid prototyping were verified with the concept of real-time interface system, and with the field programmable gate array (FPGA) board, the vibration and noise experimental analysis of the brushless direct current (DC) motor was carried out to achieve the optimization effect.

In summary, the research on electromagnetic vibration and noise reduction methods of permanent magnet synchronous motors is mainly focused on improving the pole-slot matching, changing the pole arc coefficient, optimizing the structure of the stator tooth tip [15–17], as well as the rotor slanted pole [18], later active noise control methods [19, 20], etc. As for the influence of the rotor slit structure on the electromagnetic vibration and noise of permanent magnet synchronous motors, there is little research currently. Synchronous motors with a “V” type permanent magnet structure have been widely used in the field of electric vehicles due to their simple structure and high efficiency. Therefore, the study of electromagnetic vibration and noise for this type of motor is of certain significance.

This article takes a 90 kW built-in “V” type permanent magnet synchronous drive motor as the research object. Through theoretical analysis, it is concluded that the main reason for the electromagnetic vibration of the permanent magnet synchronous motor is the imbalance of the radial electromagnetic force, which needs to be optimized. The finite element method is used to calculate the vibration and noise characteristics of the motor, and then the rotor slit structure is optimized to improve the motor magnetic field and reduce the motor’s NVH level. Three different rotor slit structures were designed, compared and analyzed, and the optimal rotor slit structure in accordance with the expected effect was selected and analyzed in detail.

2. STRUCTURAL DESIGN

2.1. Basic Parameters and Models

Taking a built-in permanent magnet synchronous motor for vehicle as the research object, the prototype is an 8-pole 48-slot permanent magnet “V”-shaped permanent magnet synchronous motor. Table 1 shows the basic parameters of the motor. According to the basic parameters of the motor, a three-dimensional model of the motor was established in the CATIA software, and reasonable simplification was carried out to facilitate the later finite element analysis and calculation. The three-dimensional model is shown in Figure 1.

Table 1. Design specification of PMSM.

parameters	value
power/	90 kW
max power	200 kW
phase	3
pole	8
rated speed	6000 (r/min)
max speed	14000 (r/min)
frequency	225 Hz
efficiency	92(%)
number of slots	48
rotor inner diameter	52 mm
rotor outer diameter	120 mm
air gap length	0.7 mm
stator inner diameter	121.4 mm
stator outer diameter	210 mm
core length	165 mm

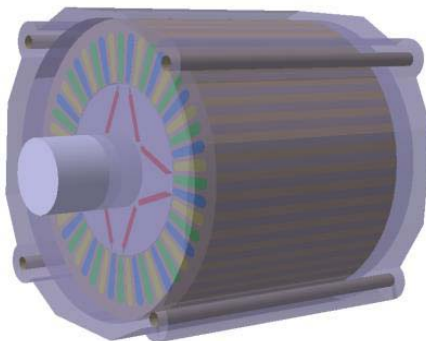


Figure 1. Motor model.

Since the main source of motor noise is electromagnetic vibration noise, and the unbalanced radial electromagnetic force during the rotation of the motor is the root cause of the electromagnetic vibration noise of the motor, if one wants to study the electromagnetic vibration and noise of the motor, one must first perform theoretical calculation and analysis on the radial electromagnetic force of the motor magnetic field. According to Maxwell Stress Tensor Method (MSTM) theory, the radial electromagnetic

force density on the stator tooth surface can be known. f_r (The unit is N/m²) is given as

$$f_r = \frac{1}{2\mu_0} (B_r^2 - B_t^2) \quad (1)$$

where B_r and B_s are the radial and tangential components of the motor air gap magnetic flux density, unit: T. B_t is the tangential component of the motor air gap magnetic flux density, unit: T. μ_0 is the vacuum permeability. The size is $4\pi \times 10^{-7}$ H/m.

The magnetic permeability of ferromagnetic materials is far greater than that of air, and the magnetic field lines are basically perpendicular to the surface of the iron core when they enter the stator and rotor cores. Therefore, the tangential air gap magnetic density is much smaller than the radial air gap magnetic density, which can be ignored. The radial electromagnetic force of the stator core structure is approximately

$$f_r = \frac{B_r^2}{2\mu_0} \quad (2)$$

The magnetic flux density at the air gap of the motor is mainly composed of the magnetic density produced by the rotor permanent magnetomotive force at the air gap, and the magnetic density is produced by the stator armature reaction magnetomotive force at the air gap.

$$B_r = B_{r\delta} + B_{s\delta} \quad (3)$$

And

$$B_{r\delta} = F_R \lambda_\delta \quad (4)$$

$$B_{s\delta} = F_S \lambda_\delta \quad (5)$$

F_R is the permanent magnetic field air gap magnetomotive force, and F_S is the stator armature reaction magnetomotive force. λ_δ is the equivalent air gap permeance.

$$F_R = \sum_{\nu_R} F_{Rm}^{\nu_R} \cos \nu_R(p\theta - \omega t) \quad (6)$$

$$F_S = \sum_{\mu} \sum_{\nu_S} F_{m\varphi}^{\mu, \nu_S} \cos(\nu_S p \theta - \mu \omega t + \varphi^{\mu, \nu_S}) \quad (7)$$

$$\lambda_\delta = \lambda_0 + \sum_{k_z}^{\infty} \lambda_{k_z} \cos k_z z_0 \theta? \quad k_z = 1, 2, 3... \quad (8)$$

where $F_{Rm}^{\nu_R}$ is the vice air gap harmonic magnetic potential amplitude. ν_R is the rotor permanent magnet magnetic field harmonic order, $2k + 1$ ($k = 0, 1, 2, \dots$). p is the number of pole pairs of the motor. θ is the mechanical angle of the rotor, rad. t is the time, s. μ is the harmonic order of the three-phase symmetrical current through the stator winding, $6k_\mu + 1$ ($k_\mu = 0, 1, 2, \dots$). S is the harmonic order of the armature reaction magnetic field, $6 + 1k_S$ ($k_S = 0, \pm 1, \pm 2, \dots$). Its absolute value represents the harmonic magnetic field order, and the positive and negative signs respectively indicate the positive rotation of the harmonic magnetic field, reverse rotation. $F_{m\varphi}^{\mu, \nu_S}$ is the amplitude of the harmonic magnetomotive force generated by the stator current, A. φ^{μ, ν_S} is the initial phase angle of the magnetomotive force, rad. λ_0 is the average permeance of the air gap, H⁻¹. k_z is the order of tooth harmonics. λ_{k_z} is the amplitude of the air gap k_z order harmonic permeance.

Substituting Equations (3), (4), (5), (6), (7), (8) into Equation (2) and expanding, after sorting out, the frequency of the radial electromagnetic force can be obtained as $(\nu_R \pm 1)f_1$, where f_1 is the fundamental electric frequency of the motor, and each order is $(\nu_R \pm \nu_S)p$, $(\nu_R \pm \nu_S)p \pm Z$, and $(\nu_R \pm \nu_S)p \pm 2Z$.

The low-order radial electromagnetic force has a very high electromagnetic force wave, which often causes greater vibration and noise. When the order is increased, the amplitude of the electromagnetic force wave is already very small, and the impact is even negligible.

3. STRUCTURE OPTIMIZATION

In order to improve the electromagnetic vibration and noise of the motor, the amplitude of the radial electromagnetic force f_r of the motor must be reduced. It can be seen from formula (3) that the radial air gap flux density $B_{r\delta}$ and $B_{s\delta}$ determine the magnitude of the electromagnetic force, and if the magnetic circuit inside the motor is changed, the radial flux density of the motor will be affected. Therefore, this paper designs three types of rotor narrow slot structure which optimizes the direction of the magnetic circuit of the motor. The structure of the motor under the specific optimization scheme is shown in Figure 2. The optimized rotor structure is named “C”, “T”, and “V” types. The unoptimized rotor is named “Basic” type.

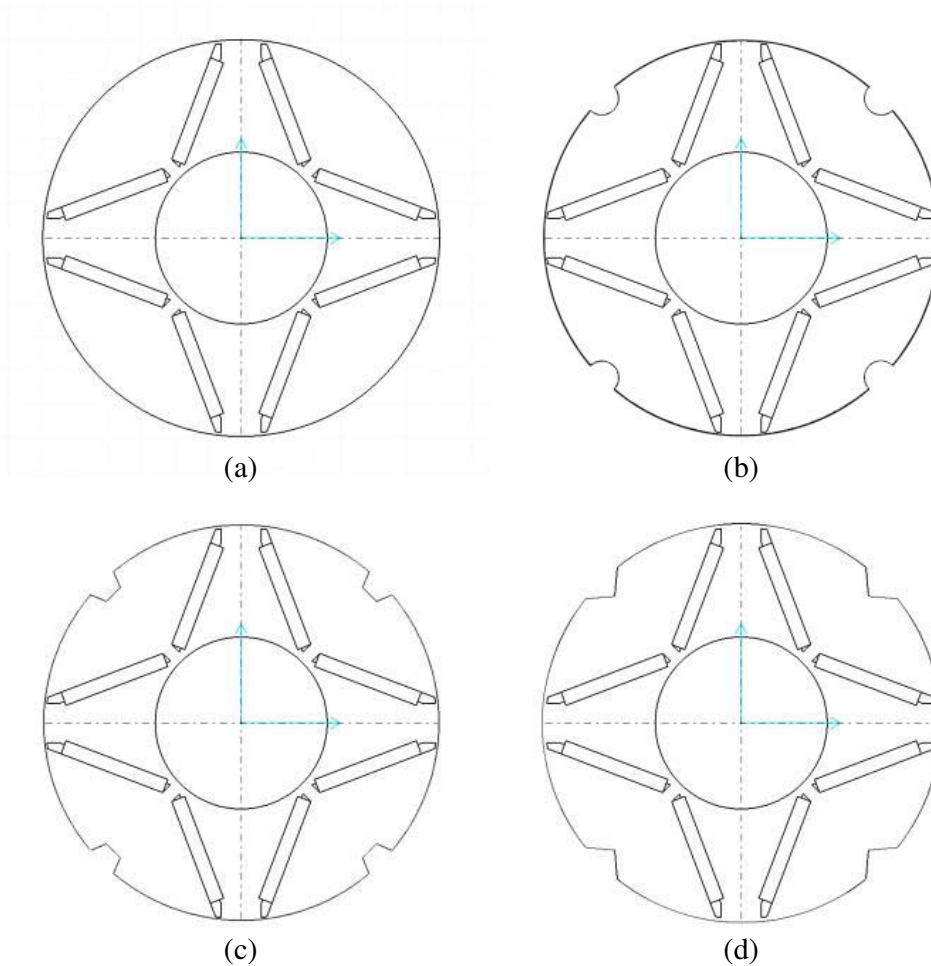


Figure 2. Four types of rotor structure. (a) “basic” type, (b) “C” type, (c) “T” type, (d) “V” type.

The rotor slit structure is optimized on the basis of the original structure and changes the direction of the magnetic circuit to varying degrees, thereby increasing the reluctance of the motor and reducing the equivalent magnetic gap of the motor.

At the same time, this rotor slit structure will reduce the mechanical strength of the rotor to a certain extent, so the mechanical strength is checked. The rotor material is silicon steel sheet, and its yield strength is 405 MPa. The stress analysis of the three optimized rotors is carried out. If the stress generated by the rotor in the rotating state is less than its yield limit, the mechanical strength can be guaranteed to meet the requirements.

4. MAGNETIC FIELD ANALYSIS

The rotor slit structure designed by CATIA can be imported into Maxwell software to analyze the magnetic field of the motor containing the rotor slit structure. The analysis results are shown in Figure 3 and Figure 4. Figure 3 is the magnetic density cloud diagram of the motor. It can be seen from the figure that the three different rotor slit structures increase the reluctance of the motor and achieve the purpose of changing the direction of the magnetic circuit in the motor to varying degrees.

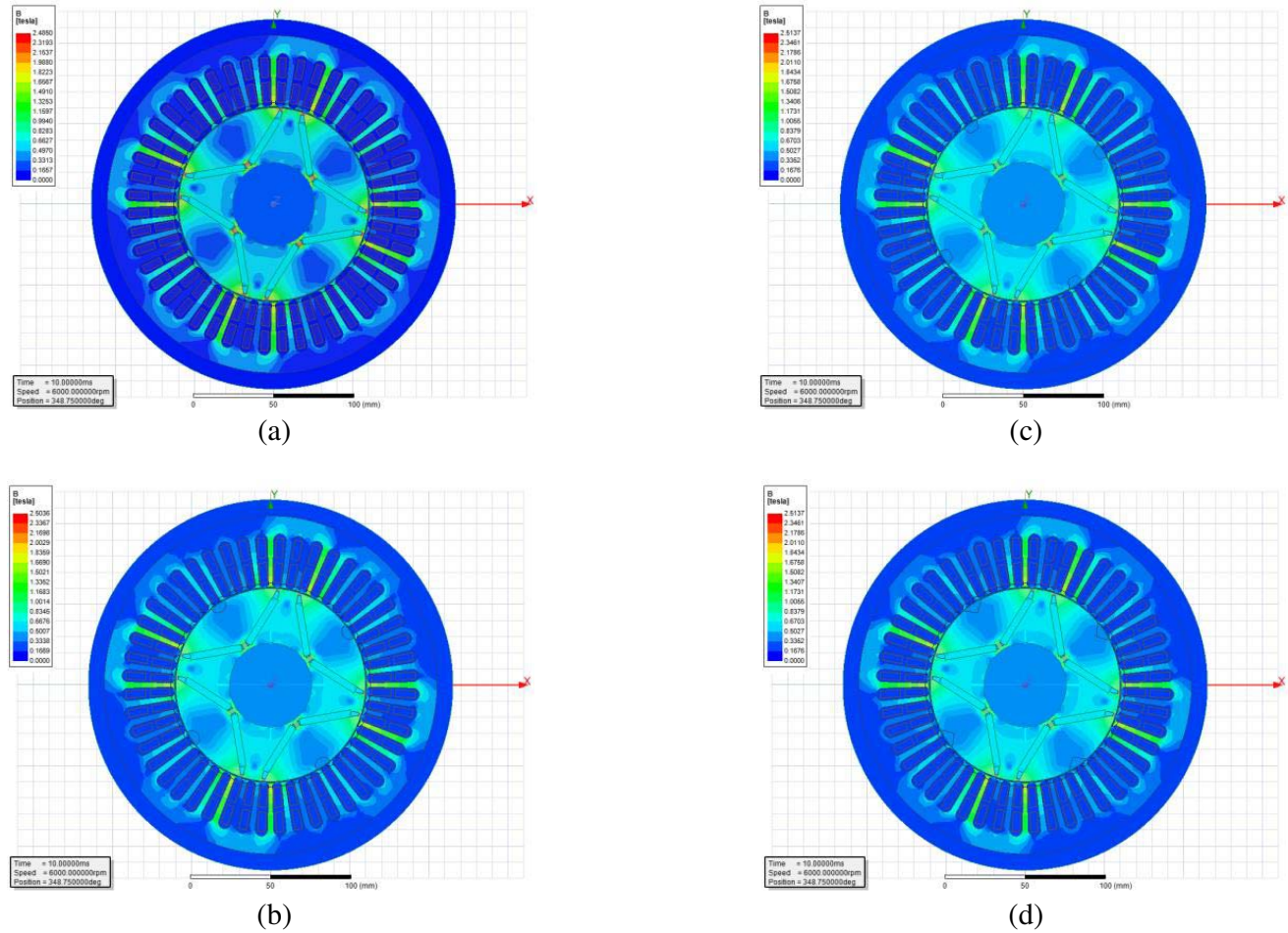


Figure 3. Magnetic flux cloud diagram under four different structures. (a) “basic” type, (b) “C” type, (c) “T” type, (d) “V” type.

However, the magnetic flux cloud diagram can only see that the magnetic circuit in the motor has changed, but it cannot directly prove the electromagnetic vibration effect of the rotor slit structure on the motor. Figure 4 is the torque change diagram of the motor. The torque on the torque diagram is the tangential torque of the motor, which will not cause motor vibration and noise under stable working conditions. It can be seen that three types of optimized motors are proposed for the slit structure, and the torque ripple in the 0–2 ms stage is significantly reduced, which can reduce the abnormal noise of the tangential torque ripple of the motor in the starting phase. In addition, during the stable working phase of the motor, it can be seen that the amplitude, torque fluctuation, and frequency of the four lines are basically the same. Therefore, the slit structure will not affect the output power of the motor under the premise of changing the direction of the motor magnetic circuit, and it will not affect the output performance of the motor.

Figure 5 is a waveforms of the induced electromotive force of a certain phase of the each structure.

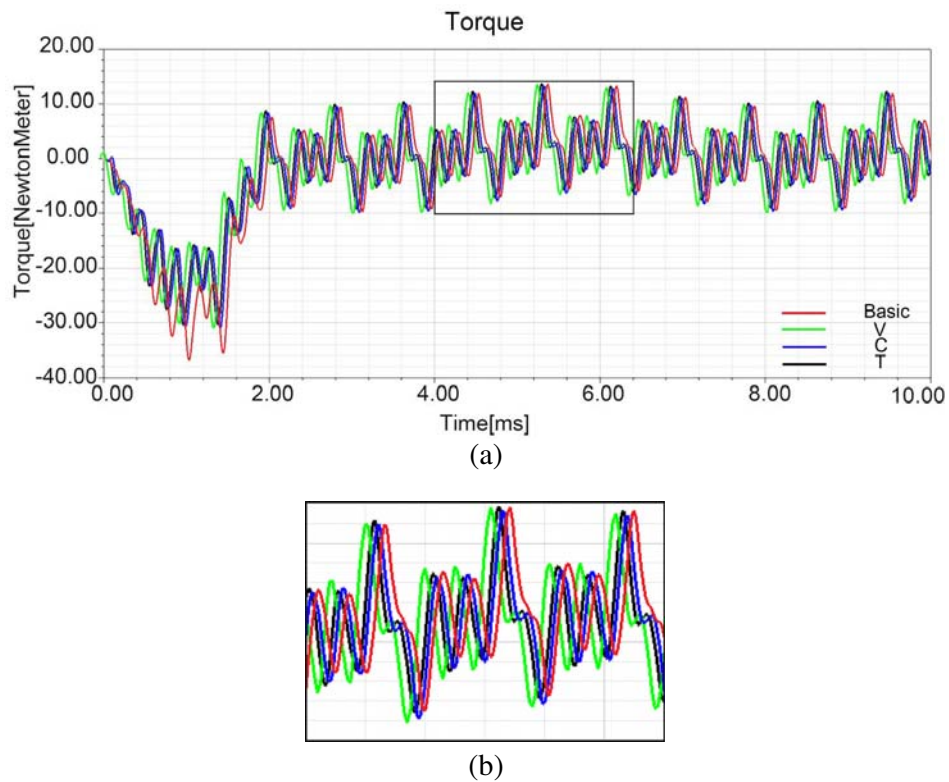


Figure 4. Torque change graph. (a) Torque change diagram under four different structures. (b) Partial enlarged view.

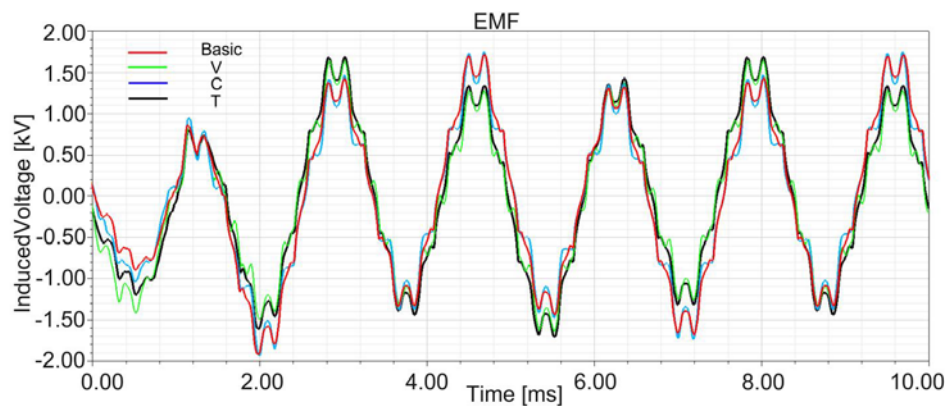


Figure 5. Waveforms of induced electromotive force EMF.

Comparing the four simulation results, the amplitudes of the four induced electromotive forces are similar, but the T-type motor has the smallest induced electromotive force fluctuation during the start-up phase and the best effect.

5. ELECTROMAGNETIC NOISE ANALYSIS

The spherical radiation model is used to simulate the electromagnetic noise of the motor, and the ANSYS workbench is used to build the motor acoustic simulation model. As shown in Figure 6, the acoustic calculation simulation needs to extract the outer surface of the motor structure and form an

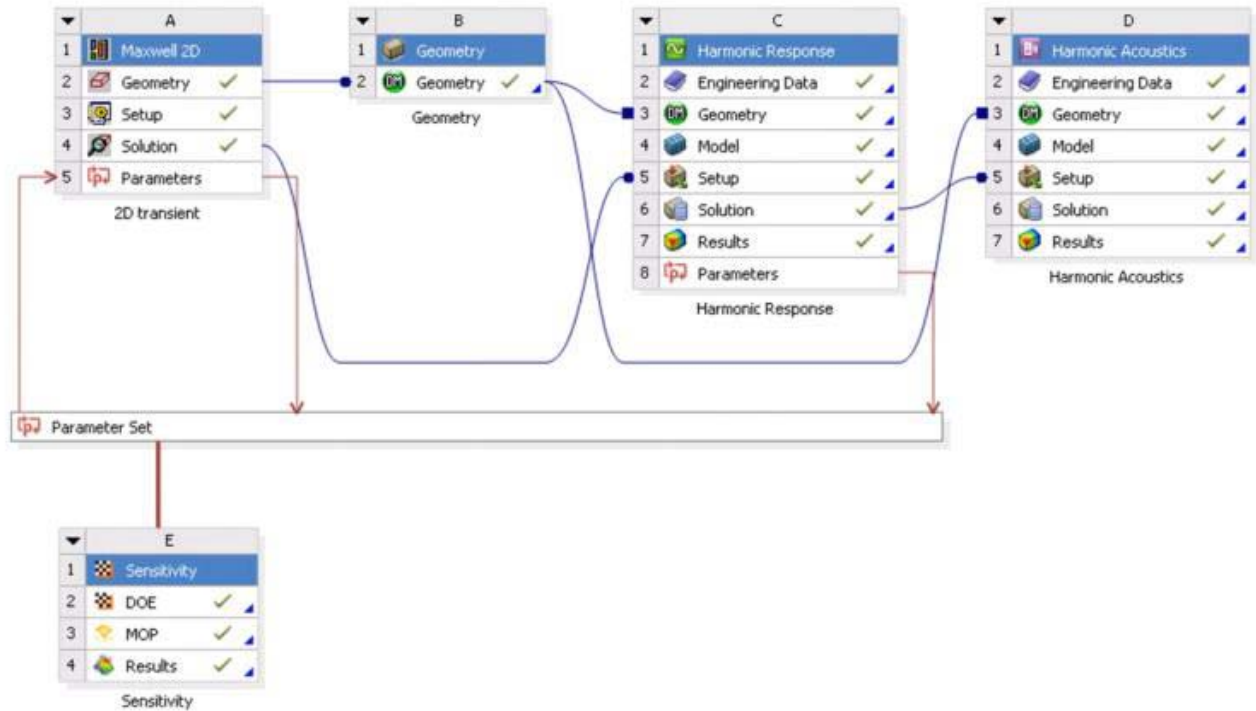


Figure 6. Simulation process.

envelope surface, and then generate near-field acoustic calculations on this basis domain grid [21].

In response to the requirements of acoustic analysis, the calculation domain is divided into one volume and two areas. The volume is established for the needs of sound radiation and sound propagation calculations, and the internal area is the outer surface of the motor structure loaded with the vibration calculation results. And the outside is required for the definition of infinite elements, simulating the conditions of the free field, and defining the fluid that is the sound propagation medium as air for calculation. Through simulation calculation, the sound pressure level (SPL) cloud diagrams of three motors with a rotor slit structure and prototypes are obtained, as shown in Figure 7.

From the sound pressure level (SPL) cloud diagrams of the four analysis results in Figure 7, comparative analysis shows that the three rotor slit structures all reduce the maximum electromagnetic noise of the motor to varying degrees. However, the reduction effect of the “C” and “V” rotor slits is not obvious, and the maximum electromagnetic noise is only reduced by less than 3 dB. The “T”-shaped rotor slit structure has an obvious effect, reducing the electromagnetic noise from 78.393 dB before optimization to 68.582 dB after optimization, a 12.5% reduction, which meets the design requirements.

By observing the SPL curve of the “T”-shaped rotor slit structure motor and the prototype at rated speed, as shown in Figure 8, the overall reduction in noise amplitude after optimization can further prove the above results. Comparing the graphs before and after optimization, the amplitude of the vibration component decreases to varying degrees at most frequencies. The sound pressure level values of the observation points are relatively large at 1000 Hz, 1800 Hz, 2400 Hz, 3200 Hz, and 3800 Hz. From the context analysis, it is known that the electromagnetic force amplitude at these frequency points is relatively large, causing large vibration acceleration. Among them, at 1000 Hz, the sound pressure level of the prototype reached the first peak of 60.31 dB, and the sound pressure level of the optimized “T” rotor slit structure motor dropped to 41.65 dB, a drop of 30.9%. At 1800 Hz, the sound pressure level of the prototype reaches the peak point of the entire curve, which is 61.996 dB, and the sound pressure level of the optimized “T” rotor slit structure motor is also effectively suppressed, which is 76.73 dB, which is down 24.7%.

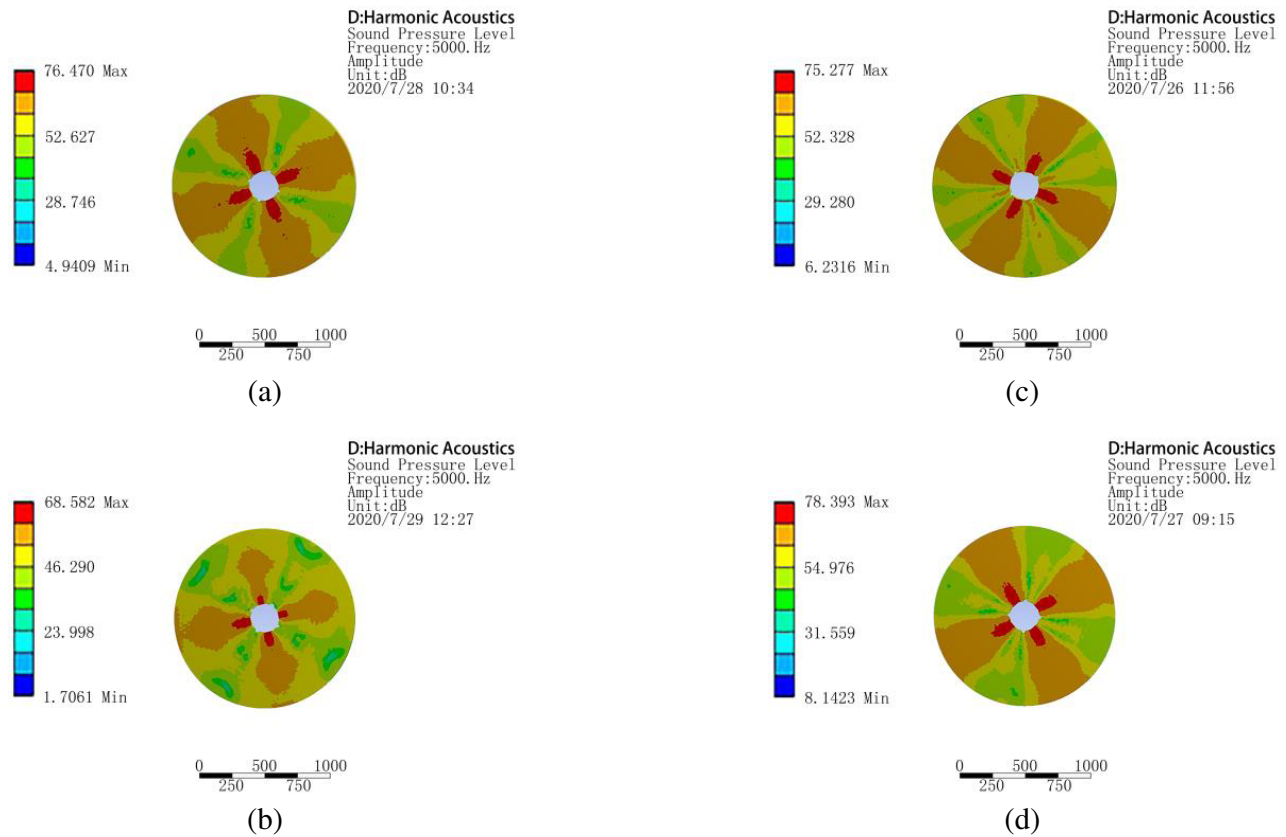


Figure 7. Noise sound pressure level cloud chart. (a) “C” sound pressure level cloud chart, (b) “T” sound pressure level cloud chart, (c) “V” sound pressure level cloud chart, (d) “basic” sound pressure level cloud chart.

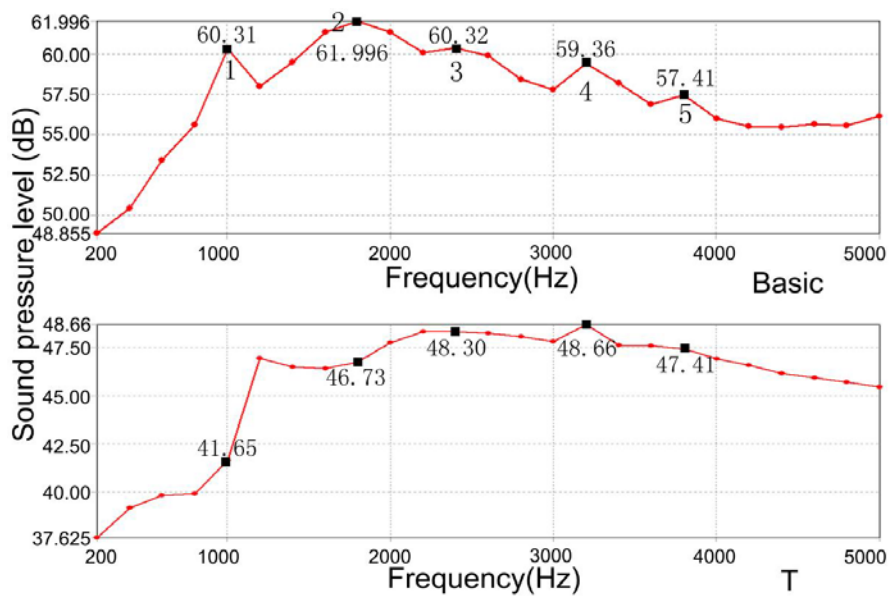


Figure 8. Sound pressure level graph.

6. CONCLUSION

This research is aimed at a permanent magnet synchronous motor for electric vehicle driving, combined with ANSYS workbench multiphysics finite element analysis platform, to study the electromagnetic noise characteristics of the motor before and after structural optimization.

Through theoretical analysis, it is concluded that the radial electromagnetic force of the motor is closely related to the electromagnetic vibration and noise of the motor. The radial electromagnetic force of the motor is determined by the radial air gap electromagnetic density. The rotor slot optimization scheme can reduce the density of the radial electromagnetic force of the motor, so as to reduce the amplitude of the radial electromagnetic force and reduce the vibration.

In order to optimize the magnetic field, three different rotor slot structures are compared with the structure before optimization. From the magnetic field, noise field, and electromagnetic force, the most suitable optimization scheme of rotor slot structure is found. By comparing the results before and after optimization, it can be seen that the optimized motor effectively reduces the motor vibration and noise, and ensures the electromagnetic performance of the motor. At 1000 Hz, the sound pressure level is reduced by 30.9%, which meets the previous design requirements.

ACKNOWLEDGMENT

This work is supported by the Natural Science Foundation of Fujian Province of China (2018J01511) and the Program for New Century Excellent Talents in Fujian Province University (2018047).

CONFLICT OF INTEREST

The authors declare no conflict of interest.

REFERENCES

1. Wang, Q., P. P. Zhao, and X. B. Du, "Electromagnetic vibration analysis and slot-pole structural optimization for a novel integrated permanent magnet in-wheel motor," *Energies*, Vol. 13, No. 13, 3488, 2020.
2. Li, J., K. Wang, and F. Li, "Analytical prediction of optimal split ratio of consequent-pole permanent magnet machines," *IET Electric Power Applications*, Vol. 3, No. 12, 365–372, 2017.
3. Zhu, X.-F., W. Hua, and Z.-Z. Wu, "Cogging torque minimisation in FSPM machines by right-angle-based tooth chamfering technique," *IET Electric Power Applications*, Vol. 5, No. 12, 627–634, 2018.
4. Jafarboland, M. and H. B. Farahabadi, "Optimum design of the stator parameters for noise and vibration reduction in BLDC motor," *The Institution of Engineering and Technology*, Vol. 12, No. 9, 1297–1305, 2018.
5. Zhu, X.-F., W. Hua, and G. Zhang, "Analysis and reduction of cogging torque for flux-switching permanent magnet machines," *IEEE Transactions on Industry Applications*, Vol. 6, No. 55, 5854–5864, 2019.
6. Lee, C.-M., H.-S. Seol, J.-Y. Lee, and D.-W. Kang, "Optimization of vibration and noise characteristics of skewed permanent brushless direct current motor," *IEEE Transactions on Magnetics*, Vol. 53, No. 11, 1–5, 2017.
7. Lin, F., S.-G. Zuo, W.-Z. Deng, and S.-L. Wu, "Reduction of vibration and acoustic noise in permanent magnet synchronous motor by optimizing magnetic forces," *Journal of Sound and Vibration*, Vol. 429, 193–205, 2018.
8. Ma, C.-G., J.-M. Li, H.-C. Zhao, J.-H. Wang, X.-R. Yin, S.-G. Zuo, X.-D. Wu, and H.-F. Lu, "3-D analytical model of armature reaction field of IPMSM with multi-segmented skewed poles and multi-layered flat wire winding considering current harmonics," *IEEE ACCESS*, Vol. 8, 151116–1511124, 2020.

9. Dong, Q.-C., X.-T. Liu, H.-Z. Qi, C. Sun, and Y.-S. Wang, "Analysis and evaluation of electromagnetic vibration and noise in permanent magnet synchronous motor with rotor step skewing," *Science China-Technological Sciences*, Vol. 62, No. 5, 839–848, 2019.
10. Lecointe, J.-P., B. Cassoret, and J.-F. Brudny, "Distinction of toothing and saturation effects on magnetic noise of induction motors," *Progress In Electromagnetics Research*, Vol. 112, 125–137, 2011.
11. Zhang, W.-T., Y.-X. Xu, H.-D. Huang, and J. B. Zuo, "Vibration reduction for dual-branch three-phase permanent magnet synchronous motor with carrier phase-shift technique," *IEEE Transactions on Power Electronics*, Vol. 35, No. 1, 607–618, 2020.
12. Hara, T., T. Ajima, Y. Tanabe, M. Watanabe, K. Hoshino, and K. Oyama, "Analysis of vibration and noise in permanent magnet synchronous motors with distributed winding for the PWM method," *IEEE Transactions on Industry Applications*, Vol. 54, No. 6, 6042–6049, 2018.
13. Rifaq, M. S. and J. W. Jung, "A comprehensive review of state-of-the-art parameter estimation techniques for permanent magnet synchronous motors in wide speed range," *IEEE Transactions on Industrial Informatics*, Vol. 7, No. 16, 4747–4758, 2020.
14. Ramaiah, V. J. and S. Keerthipati, "Hybrid PWM scheme for pole-phase modulation induction motor drive using carrier-based hexagonal and octadecagonal SVPWM," *IEEE Transactions on Industrial Electronics*, Vol. 9, No. 67, 7312–7320, 2020.
15. Liu, C.-C., J.-W. Lu, Y.-H. Wang, G. Lei, J.-Z. Zhu, and Y.-G. Guo, "Techniques for reduction of the cogging torque in claw pole machines with SMC cores," *Energies*, Vol. 10, No. 10, 1541, 2017.
16. Chen, M., K.-T. Chau, C. H. T. Lee, and C.-H. Liu, "Design and analysis of a new axial-field magnetic variable gear using pole-changing permanent magnets," *Progress In Electromagnetics Research*, Vol. 153, 23–32, 2015.
17. Nobahari, A., A. Darabo, and A. Hassannia, "Various skewing arrangements and relative position of dual rotor of an axial flux induction motor, modelling and performance evaluation," *IET Electric Power Applications*, Vol. 4, No. 12, 575–580, 2018.
18. Bonthu, S. S. R., T. Bin, and S. Choi, "Optimal torque ripple reduction technique for outer rotor permanent magnet synchronous reluctance motors," *IEEE Transactions on Energy Conversion*, Vol. 3, No. 33, 1184–1192, 2018.
19. Huang, Y.-H., L.-B. Yan, F. Yang, and W.-J. Zeng, "Research on active disturbance rejection control of hybrid excitation magnetic suspension switched reluctance motor considering noise," *Progress In Electromagnetics Research M*, Vol. 93, 197–207, 2020.
20. Ruba, M., F. Jurca, L. Czumbil, D. D. Micu, C. Martis, A. Polycarpou, and R. Rizzo, "Synchronous reluctance machine geometry optimisation through a genetic algorithm based technique," *IET Electric Power Applications*, Vol. 3, No. 12, 431–438, 2018.
21. Rick, S., A. K. Putri, D. Frank, and K. Hameyer, "Hybrid acoustic model of electric vehicles: Force excitation in permanent-magnet synchronous machines," *IEEE Transactions on Industry Applications*, Vol. 52, No. 4, 2979–2987, 2016.